Critical-region measurements of the mutual-friction parameters in rotating He II

P. Mathieu, A. Serra, and Y. Simon
Groupe de Physique des Solides de l'Ecole Normale Supérieure, 24 rue Lhomond, 75231 Paris Cedex 05, France
(Received 17 February 1976)

We report measurements of the two mutual-friction parameters B and B' in rotating He II in the range of temperature from 1.75up to 6×10^{-4} K below the λ point. All results are obtained by investigating the second-sound response of a square resonator. The data previously reported in the literature reveal some marked discrepancies in the behavior of B and B' as $T\to T_\lambda$, in spite of considerable scatter above 2.1 K. In this work we attempt to describe this behavior precisely, and at the same time we extend the measurements of B' above 10^{-2} K from T_λ. Primarily because of good temperature stabilization using a second-sound controller, a close fit of both amplitude and phase of the resonance response to calculated values was possible, which greatly improved the precision of the results. Plotting B and B' as a function of the reduced temperature $\epsilon=1-T/T_\lambda$, in the temperature range $2\times10^{-4}<\epsilon<3\times10^{-2}$, we found the experimental data are well fitted by the following expressions, where $-\alpha$ is a critical exponent near $-\frac{1}{3}$: $B=be^{-\alpha}$, $B'=b'e^{-\alpha}+b'_0$ with $\alpha=0.330\pm0.015$, $b=0.470\pm0.033$, $b'=-0.34\pm0.03$, $b'_0=1.01\pm0.12$.

I. INTRODUCTION

In the hydrodynamic equations of rotating He II, as derived by Bekarevich and Khalatnikov,[1] the mutual-friction force appears in the dissipative function from very general assumptions, and is expressed with the help of three kinetic coefficients: α, β, γ.[1] The effects of the γ terms are expected to be extremely small. α and β are related, through simple expressions,[2] respectively, to the parameters B and B' first introduced by Hall and Vinen.[3]

Several attempts have been made to predict theoretically B and B' by considering the microscopic nature of the mutual-friction force.[3-5] This is generally carried out in two steps: (i) By analysis of the hydrodynamic flow around a vortex core the mutual-friction force, and therefore B and B', are related to $\sigma_\parallel$ and $\sigma_\perp$, two effective collision diameters describing the scattering of rotons by vortices. The most elaborate model on this point is without doubt the one proposed by Hall and Vinen,[3] refined by Hall,[6] and recently reexamined by Hillel, Hall and Lucas.[7] By inversion of their expressions for B and B', $\sigma_\parallel(T)$ and $\sigma_\perp(T)$ can be calculated from the experimental data for B and B'. (ii) The cross diameters $\sigma_\parallel$ and $\sigma_\perp$ are derived from a kinetic treatment of roton-vortex line collisions.[3-5]

B and B' are experimentally determined by investigation of second-sound propagation in rotating helium. The absence of any observed extra attenuation of second sound parallel to the direction of rotation confirms that $\gamma\approx0$. The coefficient B, which induces an extra attenuation in a direction perpendicular to the vortices, has been extensively measured.[3,8-11] On the other hand, B' is generally obtained using the fact that it acts, together with the Coriolis force, in coupling two degenerate modes in square[12] or cylindrical[11] cavities.

The measurements of B are in good agreement below 2.1 K, but the results close to the λ point presented by Lipa *et al.*[10] and Lucas[11] differ considerably. The results of Lipa *et al.* up to 6×10^{-4} K from T_λ suggest that B tends towards a constant value about 2.5 at the λ point, while the Lucas and Hall[11] data up to 2×10^{-3} K from T_λ seem on the contrary to indicate that B increases monotonically as $T\to T_\lambda$.

Measurements of B' in the literature stop below 10^{-2} K from T_λ, and they lack precision. According to Lucas,[11] B' becomes negative above 2.1 K in contradiction with the large positive values of B' given by Snyder and Linekin.[12] Lucas points out a possible error in the sign of the measured quantity $2-B'$ in the results of Snyder and Linekin. For example, the last point given in Ref. 12, at $T=2.156$ K is $B'=5.7\pm2.0$. In case of an error in the sign of $2-B'$ it would be $B'=-1.7$ instead of 5.7.

In this work we present measurements of both B and B' up to 6×10^{-4} K from T_λ. Our purpose is mainly (i) to state precisely the behavior of B as $T\to T_\lambda$ and (ii) to extend the measurements of B' in the same range of temperature.

II. EXPERIMENTAL ARRANGEMENT

The second-sound resonator we used in our experiments has the same geometry as the one used by Snyder and Linekin.[12] It is a parallelepiped cavity, $a\times b\times c=3.0\times3.0\times2.6$ cm^3, with $a\approx b$ as precisely as possible. The c side is along the di-

rection of rotation, i.e., parallel to the z (vertical) axis, so that the cavity has a square cross section in the x-y plane, as shown in Fig. 1. The cavity is machined from slabs of epoxy resin Araldite. One 1-mm-diam hole is drilled at the center of each horizontal cap to allow the dc heat component to escape.

Second-sound transmitters and receivers are metallic films, about 1000-Å thick, vacuum-deposited directly onto the Araldite substrates. We have at our disposal two transmitters, on the faces $x=0$ and $y=0$, which are chromium films covering the whole height c, and as wide as possible. Two lateral strips of tin form equipotential contacts, making the heat flux input uniform. In order to generate the second sound at frequency ω, one transmitter is driven at $\frac{1}{2}\omega$ by a very low-frequency synthesizer ADRET 303. Over the explored range of temperature, the fundamental resonant frequency $\omega/2\pi$ varies from about 20 to 300 Hz. The frequency stabilization is better than one part in 10^{-8}.

Several receivers, shaped as narrow vertical strips, are arranged to probe the temperature field at different points on the faces $x=a$ and $y=b$. They consist of granular (partially oxidized) Al films.[13] Such superconducting bolometers, when deposited on Araldite, have a broad transition, over several tenths of K. They are preferred to classical carbon bolometers because of their high sensitivity, their fast thermal response, and also a better controlled homogeneity.

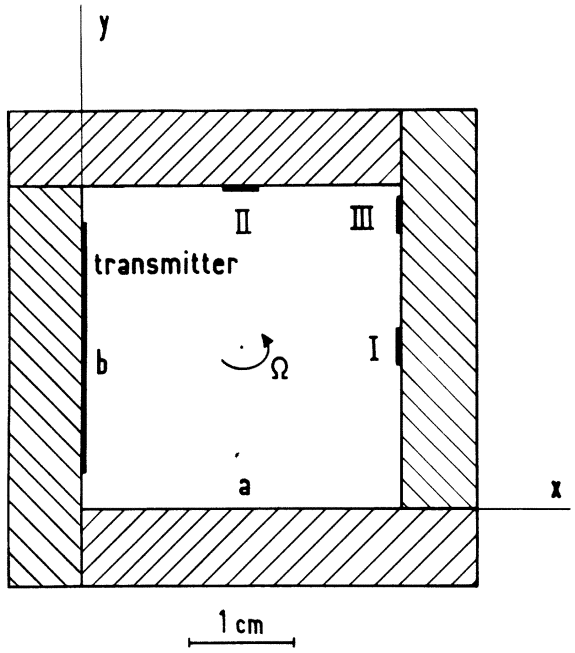

FIG. 1. Cross section of the second-sound resonator in a plane perpendicular to the rotation axis. Transmitters and receivers are metallic films ~1000 Å thick. Only the transmitter on the face $x=0$, and the three bolometers I, II, III relevant to the discussion in the text are shown in the figure. The four slabs forming the vertical walls are assembled so that $a \approx b$ as accurately as possible. The deviation from the square $|b-a|/a$ does not exceed 0.2%, as can be estimated by measuring separately the two resonant frequencies $\omega_a/2\pi$ and $\omega_b/2\pi$ at rest.

We emphasize the capability of a bolometer to measure both amplitude and phase of the temperature oscillation $T_1 e^{-i\omega t}$. We have exploited this capability extensively in our measurements. The bolometric signal is fed into a lock-in amplifier (LIA) PAR 129A. The two out-of-phase outputs of the LIA drive the two channels of an XY recorder. Thus, the complex amplitude $T_1(\omega)$ is directly plotted on the Argand diagram. Figures 2 and 3 show typical loci T_1 vs ω, obtained when varying the exciting frequency near a resonance.

Following a well-known idea,[14,15] another second-sound resonator that we refer to as the control cavity is included in a feedback loop to control the mean temperature T_0 of the helium bath. Advantage is taken of the rapid variation of phase near the resonance to get an error signal. The originality of our control system resides in the use of open glass cavities which can be driven at high harmonics with a large quality factor of the order of 15 000, which represents nearly the theoretical limit, accounting for bulk attenuation of second sound. Detailed information on the construction of such cavities will be published elsewhere,[16]

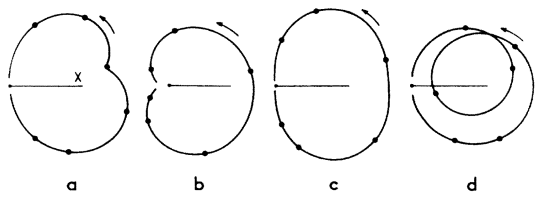

FIG. 2. First-harmonic response of the rotating cavity. Temperature $T_0 = 1.995$ K, rotational speed $|\Omega|/2\pi = 1.01$ rps. Typical X-Y recordings of the complex amplitude of the wave at bolometers I, II, or III, as function of the frequency: (a) I, clockwise (cw) rotation; (b) II, cw; (c) III, cw; (d) III, counterclockwise. It is seen that the shape of the response at bolometer III is strongly affected by the direction of rotation. From this shape the sign of the quantity $(2-B')\Omega$ can be deduced. Black dots are experimental points for a set of discrete values of the second-sound frequency: $\omega_n/2\pi = 310 + n$ Hz ($n = 0, 1, \ldots, 5$), increasing in the direction of the arrow. For clarity only six points are shown among the $N \sim 20$–60 points actually recorded. The continuous curves are those obtained by fitting all N points by an expression of the form (12). On the scale of this figure small deviations from theoretical curves cannot be appreciated.

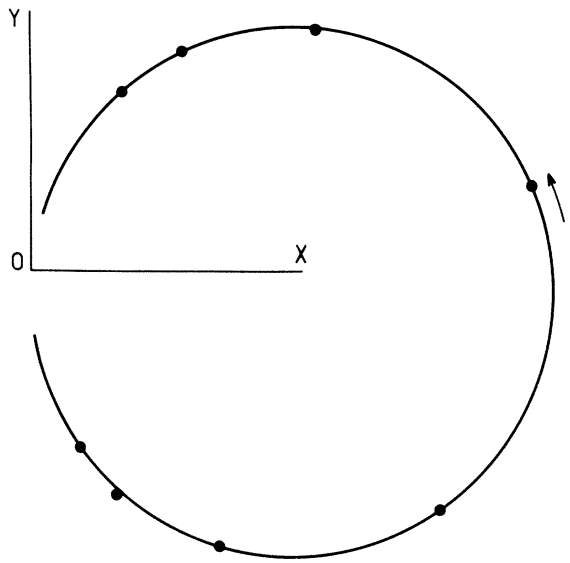

FIG. 3. Second-harmonic response of the rotating cavity. $T_0 = 2.161$ K $|\Omega|/2\pi = 1.00$ rps. Black dots: complex amplitude $X+iY$ of the wave as measured by bolometer I at frequencies $\omega_n = 195 + n$ Hz ($n = 0, 1, \ldots, 7$); ω increasing in the sense of the arrow. The resonance at even harmonics is not split, and the theoretical response curve is a circle.

together with an analysis of the feedback system and a comparative discussion of performances of second-sound controllers and conventional bridge controllers. The best registered performance, at 1.9 K and without rotation, corresponds to fluctuations less than 3×10^{-9} K in the range 0–3 Hz, during 1 h.

The control cavity and the measuring cavity are enclosed in the same box, and the whole system is rotated at a constant, positive or negative, angular velocity Ω. As the second sound in the control cavity is at a frequency 120 times that of the measuring cavity, there is no interference. In the control cavity the second sound propagates parallel to z and is not affected by rotation. On the other hand, second sound at frequencies $\gtrsim 10$ Hz regarded as a disturbance, is above the cutoff frequency of the control loop.

III. EXPERIMENTAL PRINCIPLE

Consider the rotating cavity of Fig. 1., driven at frequency ω by the transmitter of the face $x = 0$. The heat input on the transmitting face may be written as $q(y)e^{-i\omega t}$, where q equals the a-c component of the Joule effect in the chromium film, and zero elsewhere. The response of the cavity is found as a two-dimensional solution of the equations of motion,[17] where vortices are supposed to remain straight, and the z components of normal and superfluid velocity $\vec{v}_n$ and $\vec{v}_s$ are taken to be zero.

Let us recall briefly under what conditions this response is derived. We shall give in this section all material and notations needed to interpret the experimental results of Sec. IV.

If the dissipative terms associated with normal viscosity and thermal conductivity are disregarded, the linearized hydrodynamic equations set down in the rotating frame become considerably simplified. Then again, neglecting thermal expansion, first and second sound are not coupled; taking a mass flux $\vec{j} = 0$, the two-dimensional temperature field $T_1(x, y)e^{-i\omega t}$ is finally found to obey a second-sound wave equation

$$\Delta T_1 + k^2 T_1 = 0, \quad k^2 = (\omega^2/u_2^2)(1+i\beta), \tag{1}$$

where u_2 is the second-sound velocity, and $\beta(\omega, \Omega)$ is an attenuation term due to the presence of vortices. To first order Ω/ω, one has simply $\beta = B\Omega/\omega$. Note that $\beta = 0$ for $\Omega = 0$. This would give an infinite value of the quality factor Q_0 of the nonrotating cavity, which is of course not the case. There are losses, partly in the bulk but mainly in the boundary layers, which contribute to limit the value of Q_0, and are ignored in Eq. (1). If we keep, for example, in the equations of motion the term corresponding to the normal fluid thermal conductivity κ, it can be shown that it is equivalent to simply adding to Eqs. (1) and (3) a bulk attenuation term $\kappa\omega/\rho_0 C u_2^2$, where C and ρ_0 are the specific heat and mean density of He II. Boundary losses are more difficult to introduce, but we may, which is consistent with experimental results, include all losses in a single constant term β_0, such that

$$\beta = \beta_0 + B\Omega/\omega\ . \tag{2}$$

As the impedance of the walls is practically infinite compared to the characteristic impedance of helium, $Z_\infty = [\rho_0 C u_2^2]^{-1}$, the boundary conditions are obtained by equating the sources q to the inward pointing normal component $-\vec{Q}\cdot\vec{n}$ of the energy flux vector $\vec{Q}$. The expression for the energy flux in the rotating frame reduces to the single important term $T_0\sigma_0\vec{v}_n$, where σ_0 is the equilibrium value of the entropy density. Then $\vec{v}_n = -\rho_s\vec{v}_s/\rho_n$ is easily expressed as a function of T_1, yielding, always to first order in Ω/ω:

$$\vec{Q} = \alpha^{-1}[\vec{\nabla}T_1 - (i/\omega)(2-B')\vec{\Omega}\times\vec{\nabla}T_1], \tag{3}$$

with $\alpha = -i\omega z_\infty(1+i\beta)/u_2$. The boundary condition $-\vec{Q}\cdot\vec{n} = q$ implies

$$\frac{\partial T_1}{\partial n} = \alpha q - \frac{i}{\omega}(2-B')\vec{\nabla}T_1\cdot(\vec{\Omega}\times\vec{n})\ . \tag{4}$$

Noted that, except for the change of β_0 in β, the problem would be formally the same as without rotation, if the $2-B'$ term did not change the form of the boundary conditions in a fundamental way. Using the Green's function $G(\vec{r}\,|\,\vec{r}_0)$ for Eq. (1), which satisfies $\partial G/\partial n = 0$ on the walls, we can write

$$T_1 = -\iint_{\text{walls}} g(\vec{r}_0) G(\vec{r}\,|\,\vec{r}_0)\, d^3\gamma_0 \,, \tag{5}$$

where $g(\vec{r}_0)$ is the right-hand side of Eq. (4). This is a homogeneous integral equation which includes both the differential equation (1) and the boundary condition (4).

Assume now that the exciting frequency ω is varied in the neighborhood of the nth harmonic $n\omega_a = n\pi u_2/a$. As the cavity is never accurately square, the frequencies ω_a and $\omega_b = \pi u_2/b$, corresponding respectively, to the x and y fundamental modes, although very close should be considered as distinct. When interpreting small splitting effects, it may become necessary to consider the actual separation $\delta\omega = \omega_a - \omega_b$. Expanding G and T_1 in a series of normal modes and retaining only the two "resonant" terms, so that

$$T_1 = c_{n0}\cos(n\pi x/a) + c_{0n}\cos(n\pi y/b) \,, \tag{6}$$

we obtain from (5) a pair of equations which determine c_{n0} and c_{0n} as functions of ω:

$$\begin{aligned} c_{n0} &= \frac{-2/ab}{k^2 - n^2\pi^2/a^2} \\ &\quad \times\left(\alpha b q_0 - i2(2-B')\frac{\Omega}{\omega}[1-(-1)^n]c_{0n}\right), \\ c_{0n} &= \frac{-2/ab}{k^2 - n^2\pi^2/b^2} \\ &\quad \times\left(\alpha b q_n + i2(2-B')\frac{\Omega}{\omega}[1-(-1)^n]c_{n0}\right), \end{aligned} \tag{7}$$

α is defined above in Eq. (3). q_0 is the average heat input over the transmitting face, and

$$q_n = \frac{1}{b}\int_0^b q(y)\left(\cos\frac{n\pi y}{b}\right) dy.$$

We are especially interested in the first harmonic $n=1$. For a well-centered homogeneous transmitter, one has $q_1 = 0$. Solving Eq. (7) with $q_1 = 0$ and systematically neglecting the small quantities $\omega - \omega_a/\omega_a$, $\delta\omega/\omega_a$, Ω/ω, and β, compared with one, we get

$$c_{10}(\omega) = h\frac{B}{AB - \frac{1}{4}\Delta\omega^2} \,, \quad c_{01} = h\frac{-\frac{1}{2}i\Delta\omega}{AB - \frac{1}{4}\Delta\omega^2} \,, \tag{8}$$

where $A = \omega - \omega_a(1 - \frac{1}{2}i\beta)$, $B = \omega - \omega_b(1 - \frac{1}{2}i\beta)$, $h = iz_\infty q_0 u_2/a$, and $\Delta\omega$ is a small coupling term

$$\Delta\omega = (8/\pi^2)(2-B')\Omega. \tag{9}$$

Within the above-mentioned approximations Eq. (8) coincides with the expressions of c_{01} and c_{10} given by Snyder and Westerwelt.[17] Note that the sign of $\Delta\omega$, and therefore of $2-B'$ and Ω, appears only in c_{01}. The observation of the (10) mode alone cannot give any information about the sign of $2-B'$. To interpret the experimental results, it is convenient to rewrite c_{01} and c_{10} each as the sum of two terms

$$\begin{aligned} c_{10} &= \lambda_1[1 - i\gamma_1(\omega-\omega_1)]^{-1} + \lambda_2[1 - i\gamma_2(\omega-\omega_2)]^{-1}, \\ c_{01} &= \mu_1[1 - \gamma_1(\omega-\omega_1)]^{-1} + \mu_2[1 - i\gamma_2(\omega-\omega_2)]^{-1} \,, \end{aligned} \tag{10}$$

$$\begin{aligned} &\gamma_1 = 2/\beta\omega_1 \approx 2/\beta_2\omega_2 = \gamma_2, \\ &\omega_2 - \omega_1 = [\Delta\omega^2 + \delta\omega^2]^{1/2} \,. \end{aligned} \tag{11}$$

Keeping in Eq. (11) the square root with the same sign as $\Delta\omega$, ω_1 and ω_2 are two unambiguously defined frequencies symmetrically placed around $\frac{1}{2}(\omega_a + \omega_b)$. The λ_i and μ_i are weakly dependent functions of ω and are considered as constants within our approximation, while the quantities in square brackets are responsible for the strong signal variation in the resonant region. In the ideal case $a = b$, or for angular velocities large enough so that $\Delta\omega >> \delta\omega$, λ_1, λ_2, μ_1, and μ_2 are, respectively, proportional to 1, 1, i, and $-i$. There is no need to give the general expressions for λ_i and μ_i. Let us simply indicate that if $\delta\omega$ is not negligible compared with $\Delta\omega$, λ_2/λ_1 is no longer equal to unity. On the other hand, it can be readily seen from Eq. (7) that $q_1 \neq 0$ results in some mixing of the right-hand terms of Eq. (8). In this case Eq. (11) is still valid, but the λ_i and μ_i must be corrected by factors $1 \pm iq_1/q_0$ depending on the direction of rotation. Accordingly c_{10} becomes slightly dependent of the sign of Ω.

From Eq. (6) it is seen that the temperature field at any point (x, y) of the cavity, in particular, on the bolometers I, II, III indicated on Fig. 1, can be written

$$T_1 = \theta_1[1 - i\gamma_1(\omega-\omega_1)]^{-1} + \theta_2[1 - i\,\gamma_2(\omega-\omega_2)]^{-1}, \tag{12}$$

where θ_1 and θ_2 are two complex amplitudes, linear combinations of the λ_i and μ_i. Each term of Eq. (12) taken separately appears as a classical resonance response and the corresponding plot in the complex plane is a circle passing through the origin of coordinates. A resonance circle is traced counterclockwise as frequency increases. Consider, for instance, the first resonant term. The point θ_1, at $\omega = \omega_1$, corresponds to the maximum

modulus, and 45° from this point corresponds to the half-width of the common response curves. The quality factor, defined as the ratio of resonance frequency ω_1 to this half-width is simply related to γ_1 and β by

$$Q_1 = \gamma_1 \omega_1 = 2/\beta . \tag{13}$$

At a given temperature T_0 and angular velocity Ω, frequency splitting $\omega_2 - \omega_1$ and Q factors are determined, therefore, the shape of the bolometric response in the complex plane is uniquely dependent on the value of the complex ratio θ_2/θ_1. We are never very far from the ideal case, where $q_1 = 0$, $\delta\omega = 0$, with receivers precisely positioned either at the center of a face (I and II) or at a corner of the cavity (III). Values of θ_2/θ_1 in this ideal case are sufficient to show the main aspects of the recorded signals on bolometers I, II, III, as shown in Fig. 2.

Thus on the bolometer I opposite the transmitter ($x = a$, $y = \frac{1}{2}b$), ideally $T_1(\mathrm{I}) = -c_{10}$, $\theta_2/\theta_1 = 1$, and the response remains unchanged when rotation is changed from clockwise to counterclockwise. Actually, $T_1(\mathrm{I})$ is slightly affected by reversing the direction of rotation, due to unavoidable deviations from ideal conditions: (i) inhomogeneity of the transmitter ($q_1 \neq 0$) making c_{10} dependent on the sign of Ω, (ii) poor centering of the receiver rendering it sensitive to the (01) mode, (iii) or alternatively, inhomogeneity of the receiver if extended over the face $x = a$. These may account for unexplained differences in the shape of the response curves associated with the direction of rotation in the results of Snyder and Linekin.[12]

Bolometer II is set at ($x = \frac{1}{2}a$, $y = b$) in order to receive the (01) mode alone, $T_1(\mathrm{II}) = -c_{01}$, $\theta_2/\theta_1 = i/-i = -1$. Changing Ω to $-\Omega$ results in a change of π in the phase of the signal $T_1(\mathrm{II})$ without affecting its shape. As for bolometer III ($x = a$, $y = b$), $T_1(\mathrm{III}) = -(c_{10} + c_{10})$, $\theta_2/\theta_1 = 1 - i/1 + i = -i$, and the two resonance circles have diameters in quadrature. In this case the sign of $\Delta\omega$, determining which of the two frequencies ω_1 or ω_2 is the lower, strongly affects the actual shape of the response plot, as can be seen in Fig. 2. Therefore we can determine the sign of $2 - B'$ by mere inspection of a recorded plot of $T_1(\mathrm{III})$. Experimentally we found the quantity $2 - B'$ to be always positive in the whole range of temperature explored, in agreement with the conclusions of Lucas.[11]

We also observed the second harmonic $n = 2$. From Eq. (7) it is clear that the coupling effect vanishes for even harmonics. The response plot $T_1(\mathrm{I})$ remains a simple resonance circle, as verified experimentally (Fig. 3). The only effect of rotation is to decrease the amplitude of the resonance and the associated Q factor. Observing how the Q of second harmonic varies as function of Ω, we may have a straightforward method to measure B. But since a computer program is used in order to analyze split resonant responses such as those shown in Fig. 2, it turns out that both B and B' are deduced from the first harmonic satisfactorily.

IV. DATA REDUCTION AND RESULTS

As explained in Sec. II the bolometric signal is directly recorded as a complex voltage amplitude $Z = X + iY$. The general expression (12) for temperature amplitude T_1 also represents within a multiplicative complex factor the recorded signal Z. This comples factor Z/T_1 is determined by the sensitivity of the LIA and the arbitrary setting of the zero-phase axis relative to the reference signal. The method to determine the significant parameters $\omega_2 - \omega_1$, γ_1, and γ_2, consists of fitting the measured signal Z with an expression of the form (12). This procedure is obviously correct only if Z/T_1 is really a constant independent of ω. This is right as long as the thermal time constants τ's of transmitter and bolometer are negligibly small, which is true for the metallic films we use. Strictly the heater and bolometer transfer operators, involving a factor $[1 - i\omega\tau]^{-1}$, cause a frequency-dependent phase lag, first between the output of the synthesizer which supplies the reference signal to the LIA and the input q_0, and second, between T_1 and the pick-up voltage. For instance, painted carbon bolometers having τ as large as 0.3 msec would introduce a systematic error in phase of about 2° over an interval $\Delta\omega/2\pi \sim 10$ Hz. In this connection, it is even more imperative to make sure that the input amplifier of the LIA has a flat response. For instance, operating the LIA at about 100 Hz with a selective amplifier having a Q factor as low as five, the error in phase for 1 Hz would already be 6°.

Prior to any recording we always begin by making sure that the resonant response of the cavity at some given angular velocity Ω and bath temperature T_0 is perfectly linear with the heat input q_0 (modulus of Z proportional to q_0 and constant phase). To warrant a linear response, q_0 must be turned down as we approach T_λ ($q_0 \simeq 0.1$ μW/cm^2 at $T_\lambda - T \approx 5 \times 10^{-4}$ K). We did not try to precisely define a critical heating power P_c nor to systematically study P_c vs T_0. However, it is worth pointing out qualitatively that what we observed as the first critical limitation was the second-sound amplitude rather than q_0 itself or the dc heat component. When increasing Ω at fixed temperature, which increases accordingly the sound attenuation, we were allowed to turn up q_0 to retrieve the same

sound amplitude without getting out of the linear region.

After T_0 is well stabilized and a rotating equilibrium is attained and maintaining constant some suitable transmitting power, the exciting frequency is increased by steps. The response $Z(\omega)$ is plotted by points for about $N=20$ to 60 discrete values ω_n of the frequency. Over the whole range of increasing values of T_0, the amplitude of the pick-up voltage decreases from 100 μV to 100 nV. Correspondingly, the time constant of the LIA must be increased from 0.3 to 10 sec and the total duration of a run increases from 5 to 30 min. After a frequency run, to test that no significant changes of temperature, angular velocity, or transmitting power occurred during the measurements, we return to the starting frequencies to ascertain the reproducibility of the first points. As far as $T_\lambda - T \gtrsim 10^{-3}$ we detect no observable change in the points, within the precision of the recorder pen. The situation deteriorates rapidly for $T_\lambda - T < 10^{-3}$K. For the highest temperature $T_\lambda - T \simeq 5\times10^{-4}$K, variations of Z may reach 1 mm on the recording sheet, which represents about 0.5% of $|Z|$. Another reason which limits our measurements to $T_\lambda - T \sim 5\times10^{-4}$K is that above this temperature the second-sound frequency decreases under 10 Hz and falls into the bandwidth of the temperature controller. Experimental second sound becomes affected by the control system like any external disturbance.

The remarkable reproducibility of the registered points Z_n after a time of 30 min can essentially be attributed to the absence of long-term temperature drift, when regulating with a second-sound cavity, in contrast with a classical bridge controller.[16] From the well-calibrated dimensions of the control cavity and from its resonant frequencies, we obtain u_2 with a precision of 10^{-3}, and T_0 is estimated using the table value of $u_2(T)$ from Greywall and Ahlers.[18] On the other hand, Ω is measured with a precision of 0.5%.

Let us denote by $f(\omega)$ the function of frequency on the right-hand side of Eq. (12). It depends on eight parameters, viz., the real and imaginary parts of θ_1 and θ_2, ω_1, ω_2, γ_1, and γ_2. To fit a set of observed points Z_n with a function of the form $f(\omega)$ regression calculations are performed on a computer. The eight parameters in $f(\omega)$ are taken as the unknown regression coefficients, and are determined so as to minimize the sum of squares of the residuals, $\sum_n |Z_n - f(\omega_n)|^2$. Table I compares the optimized values of the quantities of interest $\omega_2 - \omega_1$, γ_1, and γ_2, as calculated from the recordings shown in Fig. 2. Note that these recordings were obtained by changing only the probe bolometer or the direction of rotation, given T_0 and $|\Omega|$. The good agreement of these results, within the estimated errors, justifies the above analysis of the second-sound wave in the cavity and gives confidence on the data reduction procedure. Note also that γ_1 and γ_2 are allowed to vary independently in the regression program. The results in each case confirm that $\gamma_1 \approx \gamma_2$ as it should be according to Eq. (11).

TABLE I. Optimized values of the quantities $\omega_2 - \omega_1/2\pi$, γ_1, and γ_2 as obtained by fitting the four recorded plots in Fig. 2 labeled *a*, *b*, *c*, and *d* to an expression of the form (12). N is the total number of points $(X_n + iY_n)$ fitted. The uncertainty in the last digit given in the parentheses corresponds to 99% confidence intervals.

Refer to Fig. 2	N	$(\omega_2-\omega_1)/2\pi$ (Hz)		$\gamma_1 = Q_1/\omega_1$ (sec)		$\gamma_2 = Q_2/\omega_2$ (sec)	
(a)	32	1.59	(5)	0.173	(5)	0.179	(6)
(b)	20	1.61	(7)	0.170	(6)	0.173	(8)
(c)	22	1.55	(5)	0.179	(8)	0.184	(9)
(d)	42	1.58	(4)	0.176	(4)	0.178	(4)

At each working temperature T_0, γ_1 (or γ_2), and $\omega_2 - \omega_1$ are measured for a few values of the rotation Ω. The plot of $1/\pi\gamma_1$ vs $\Omega/2\pi$ as shown in Fig. 4 is a straight line, in accordance with Eqs. (2) and (11):

$$1/\pi\gamma_1 = \beta_0\omega_1/2\pi + B\Omega/2\pi \,. \tag{14}$$

The extrapolated value of $1/\pi\gamma_1$ for $\Omega = 0$ is inversely proportional to the quality factor Q_0 of the cavity at rest. The slope B is computed by sim-

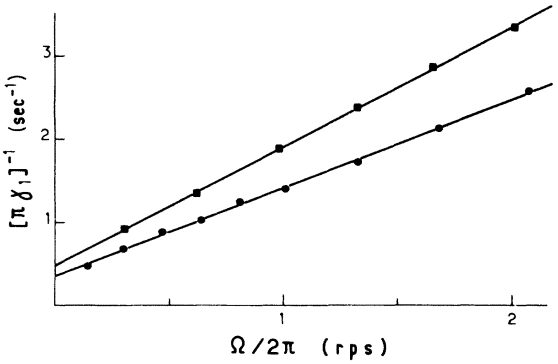

FIG. 4. Examples of plots at fixed temperature of $[\pi\gamma_1]^{-1}$ vs $\Omega/2\pi$: (●) $T = 1.995$ K, (■) $T = 2.113$ K. The quantity $[\pi\gamma_1]^{-1}$ defined in Eq. (11) is inversely proportional to the quality factor of the cavity, expresses second-sound attenuation, and increases linearly with rotational speed $\Omega/2\pi$ in accordance with Eq. (14). The fitted straight line has a slope $B(T)$ and the nonzero intercept indicates a finite quality factor at rest.

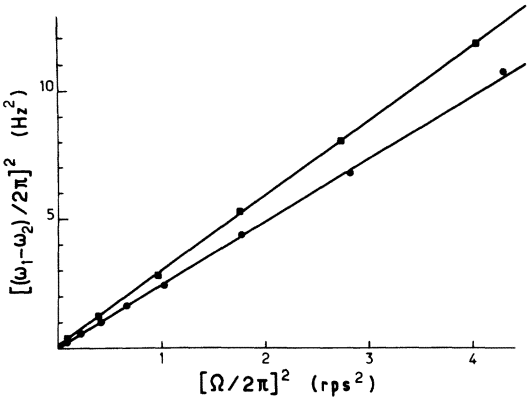

FIG. 5. Examples of plots at fixed temperature of the squared frequency splitting vs $(\Omega/2\pi)^2$: (●) $T=1.995$ K, (■) $T=2.113$ K. In accordance with Eqs. (9) and (11) the slope of the fitted line yields $|2-B'|$. As explained in the text a small nonzero intercept $(\delta\omega/2\pi)^2$ can arise because the cavity is not perfectly square, and this may randomly vary due to assembling and disassembling the cavity to change bolometers. Whereas negligible in one case (lower line), $\delta\omega/2\pi \sim 0.3$ Hz in the other (upper line).

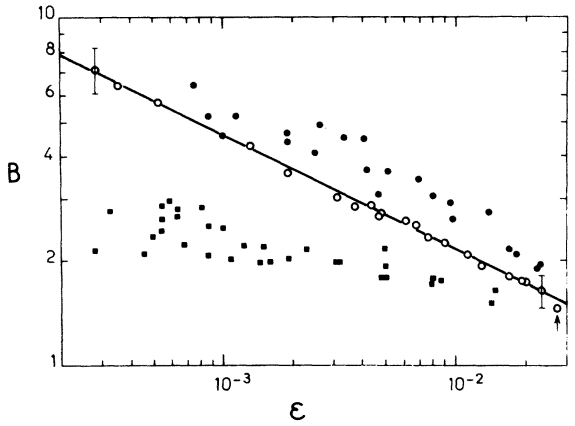

FIG. 7. Mutual-friction parameter B as a function of the reduced temperature $\epsilon=1-T/T_\lambda$ on logarithmic scales: (○) present measurements, (●) data of Lucas and Hall (Ref. 11), (■) Lipa *et al.* (Ref. 10). The fitted straight line corresponds to the power-law dependence given in the text, with critical exponent near $-\frac{1}{3}$. Typical error bars are shown at both ends of the scale.

ple linear regression. Results for $B(T)$ are collected in Figs. 6 and 7. We verified that the attenuation observed in the second harmonic is consistent with the values found for B.

As shown in Fig. 5 the squared splitting $[(\omega_1-\omega_2)/2\pi]^2$ is plotted as a function of $(\Omega/2\pi)^2$. According to Eqs. (9) and (11) the relationship between these two quantities is linear. The computed slope of the regression line is used to derive $|2-B'|$. As explained above, we can deduce the sign of $(2-B')$ by mere inspection of the response plot of bolometer II. Results for $B'(T)$ are shown in Figs. 8 and 9. Any observed nonzero intercept of the line $[(\omega_1-\omega_2)/2\pi]^2$ vs $(\Omega/2\pi)^2$ clearly corresponds to a nonzero separation $\delta\omega$, as estimated at rest from the measured values of ω_a and ω_b. It should not be confused with the unexplained nonzero intercept that Snyder and Linekin observe in plotting the separation of the maxima of their response curve Δf as a function of the rotational velocity.[12]

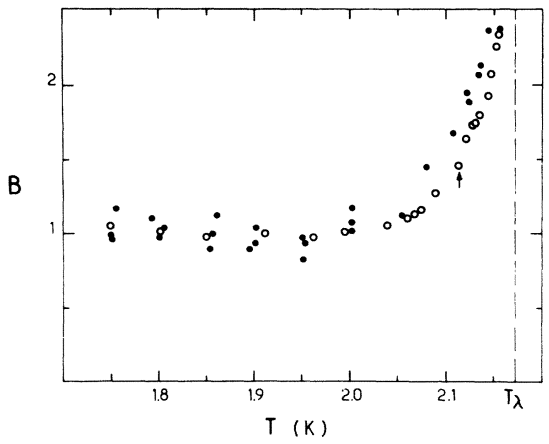

FIG. 6. Temperature dependence of the mutual-friction parameter B above 1.75 K. Experimental points: (○) present measurements, (●) data of Lucas from Ref. 11. The arrow marks the first point shown again in Fig. 7.

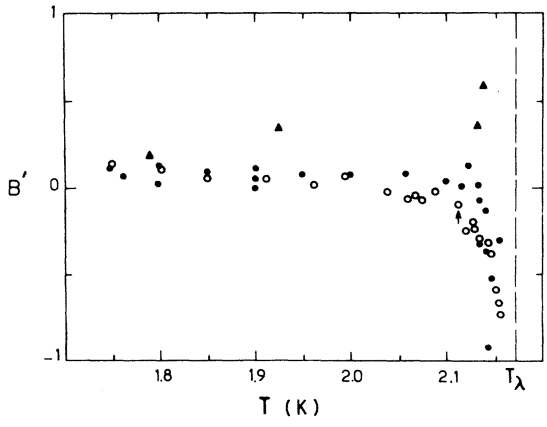

FIG. 8. Temperature dependence of the mutual-friction parameter B': (○) present measurements, (●) Lucas (Ref. 11), (▲) Snyder and Linekin (Ref. 12). The arrow marks the first point reported in Fig. 9.

V. CONCLUSION

Our results for B agree well with the measurements of the previous authors in the lowest investigated range of temperature, $1.75 < T < 2.10$ K. In Fig. 6 they are compared in particular with the data from Lucas. Above 2.1 K values from Lucas and Hall[11] become systematically greater than ours, while those from Lipa *et al.*[10] remain markedly lower. This appears clearly in Fig. 7 where B is plotted versus the dimensionless parameter $\epsilon = 1 - T/T_\lambda$ using logarithmic scales, over the range $2\times10^{-4} < \epsilon < 3\times10^{-2}$. It is clear from this plot that B can be described in this range by a power law of the form

$$B = b\epsilon^{-\alpha} . \tag{15}$$

The two parameters b and α determined by a least-squares method are found to be

$$b = 0.470 \pm 0.033, \quad \alpha = 0.330 \pm 0.015 .$$

Our results for B' confirm the observations of Lucas[11] over the common range of temperature (Fig. 8); in particular, the existence of a negative divergence, which excludes the large positive values found by Snyder and Linekin.[12] This agreement is especially conclusive as we have used a geometry and method very similar to that of Snyder and Linekin. Results in the range $2\times10^{-4} < \epsilon < 3\times10^{-2}$ are reported in Fig. 9. Clearly, B' can no longer be described by a simple expression like (15), as B' is already near zero at $\epsilon = 3\times10^{-2}$, and yet the experimental data in this temperature range are correctly fitted by an expression of the form

$$B' = b'\epsilon^{-\alpha} + b_0' , \tag{16}$$

with

$$b' = -0.34 \pm 0.03, \quad b_0' = 1.01 \pm 0.12,$$

α being the same exponent as for B. In Fig. 9, $b_0' - B$ is plotted as a function of ϵ in log-log scales, using this best estimate of b_0', $b_0' = 1.01$. The best fit [Eq. (16)] then appears as a straight line with slope $-\alpha$.

As our measurements of both B and B' agree well with those of Lucas in the intermediate temperature range of $1.75 < T < 2.10$ K, we may

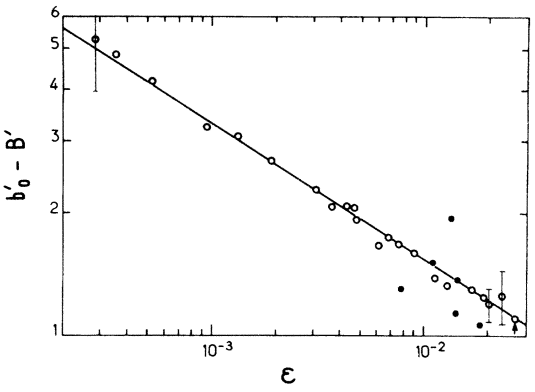

FIG. 9. The quantity $b_0' - B'$, where $b_0' = 1.01$ is plotted as a function of the reduced temperature $\epsilon = 1 - T/T_\lambda$: (○) present measurements, (●) Lucas (Ref. 11). The constant b_0' and the solid straight line have been fitted as described in the text.

adopt Lucas's discussion of the comparison with theory. We refer in particular to the recent article by Hillel, Hall, and Lucas,[7] where the authors recalculated the cross diameters $\sigma_\parallel$ and $\sigma_\perp$ from Lucas's results and compared them with theoretical values. From this comparison it is obvious that none of the existing theories is able to account for the behavior of B and B' above 1.7 K.

As pointed out also by Hillel *et al.* the values of $\sigma_\parallel$ and $\sigma_\perp$ close to T_λ are quite insensitive to the experimental scatter in B and B' as $T \to T_\lambda$. Provided only that $B \to +\infty$ and $B' \to -\infty$, the asymptotic values of $\sigma_\parallel$ and $\sigma_\perp$ are determined: $\sigma_\perp \to 7.4$ Å, $\sigma_\parallel \to 0$. Even the limiting behavior of $\sigma_\perp$, $\sigma_\perp \approx 7.4(1 + \rho_s/\rho)$, does not depend on the critical exponents of B and B'. The only point we may infer, in the theoretical scheme of Hillel *et al.*, concerns the limiting behavior of $\sigma_\parallel$. Taking a critical exponent $\alpha = -\frac{1}{3}$ for B and B', and knowing $\rho_s \propto \epsilon^{2/3}$, it is found that $\sigma_\parallel \to 0$ like ϵ.

Whether or not[5] the hydrodynamic analysis of Hillel *et al.* is adopted as a first step, the theory of mutual-friction coefficients near the λ point remains to be completed. The most marked feature of our measurements, the result that such a theory should have to justify, is in our opinion the evidence of a critical exponent for B and B', with a value near $-\frac{1}{3}$.

[1]I. L. Bekarevich and I. M. Khalatnikov, Zh. Eksp. Teor. Fiz. 40, 920 (1961) [Sov. Phys.-JETP 13, 643 (1961)].
[2]I. M. Khalatnikov, *Introduction to the Theory of Superfluidity* (Benjamin, New York, 1965), Chap. 16.
[3]H. E. Hall and W. F. Vinen, Proc. R. Soc. A 238, 204 (1956); 238, 215 (1956).
[4]E. M. Lifshitz and L. P. Pitaevskii, Zh. Eksp. Teor. Fiz. 33, 535 (1957) [Sov. Phys.-JETP 6, 418 (1958)].
[5]S. E. Goodman, Phys. Fluids 14, 1293 (1971).
[6]H. E. Hall, J. Phys. C 3, 1166 (1970).
[7]A. J. Hillel, H. E. Hall, and P. Lucas, J. Phys. C 7, 3341 (1974).
[8]H. A. Snyder and Z. Putney, Phys. Rev. 150, 110 (1966).
[9]P. J. Bendt, Phys. Rev. 153, 280 (1967).

[10]J. A. Lipa, C. J. Pearce, and P. D. Jarman, Phys. Rev. 155, 75 (1967).
[11]P. Lucas, J. Phys. C 3, 1180 (1970).
[12]H. A. Snyder and D. M. Linekin, Phys. Rev. 147, 131 (1966).
[13]R. W. Cohen and B. Abeles, Phys. Rev. 168, 44 (1968).
[14]J. A. Tyson and D. H. Douglass, Jr., in *Proceedings of the Eleventh International Conference on Low Temperature Physics*, edited by J. F. Allen, D. M. Finlayson, and D. M. McCall (University of St. Andrews Printing Dept., St. Andrews, Scotland, 1969), p. 215.
[15]M. François, Cryogenics 15, 573 (1975).
[16]J. C. Maréchal and P. Mathieu (unpublished).
[17]H. A. Snyder and P. J. Westerwelt, Ann. Phys. (N.Y.) 43, 158 (1967).
[18]D. S. Greywall and G. Ahlers, Phys. Rev. A 7, 2145 (1973).